Coexistence and Criticality in Size-Asymmetric Hard-Core Electrolytes

José Manuel Romero-Enrique,* G. Orkoulas, Athanassios Z. Panagiotopoulos,† and Michael E. Fisher
Institute for Physical Science and Technology, University of Maryland, College Park, Maryland 20742-2431
(Received 28 July 2000)

Liquid-vapor coexistence curves and critical parameters for hard-core 1:1 electrolyte models with diameter ratios $\lambda = \sigma_-/\sigma_+ = 1$ to 5.7 have been studied by fine-discretization Monte Carlo methods. Normalizing via the length scale $\sigma_\pm = \frac{1}{2}(\sigma_+ + \sigma_-)$, relevant for the low densities in question, both T_c^* $(= k_B T_c \sigma_\pm/q^2)$ and ρ_c^* $(= \rho_c \sigma_\pm^3)$ decrease rapidly (from $\simeq$0.05 to 0.03 and 0.08 to 0.04, respectively) as λ increases. These trends, which unequivocally contradict current theories, are closely mirrored by results for tightly tethered dipolar dimers (with T_c^* lower by $\sim$0%$-$11% and ρ_c^* greater by 37%$-$12%).

PACS numbers: 64.70.Fx, 02.70.Lq, 05.70.Jk

The formation of coexisting fluid phases of different electrolyte concentrations in ionic solutions has been the topic of numerous recent experimental [1], theoretical [2,3], and simulation studies [4–7]. The simplest models for electrolytes—the "primitive models"—treat the solvent as a uniform dielectric continuum. The most studied system is the restricted primitive model (RPM) that consists of equisized hard spheres, half carrying a charge $+q$ and half $-q$. Recent simulations [4–7] agree with respect to the critical temperature and density for the vapor-liquid transition, finding the remarkably low values $T_c^* \simeq 0.05$ and $\rho_c^* \simeq 0.07$ [6]; see (1). By contrast to the RPM, the effects of charge and size asymmetry have not been extensively analyzed either theoretically or via simulation.

Here we focus on the effects of *size asymmetry* on gas-liquid coexistence and critical parameters by studying hard-core primitive models for 1:1 electrolytes that have *no restrictions* on the relative magnitude of the diameters of the + and − ions, i.e., the so-called size-asymmetric primitive model [3]. The first claim to treat size asymmetry theoretically appears already in Debye and Hückel's original paper [8,9] and extensions invoking Bjerrum ion pairing have been analyzed [9]. Other mean potential approaches include the symmetrized Poisson-Bolzmann and modified Poisson-Boltzmann [10] schemes. The mean spherical approximation (MSA) [2,3,10] and hypernetted-chain [11] integral equations have also been applied. Currently, however, there are no simulation results available to check these various theories.

This work, which extends [12], provides a first study of the effects of size asymmetry on both critical parameters and liquid-vapor coexistence [13]. We find, in fact, a systematic trend of T_c and ρ_c with increasing size asymmetry that directly conflicts with the principal theories cited.

To be specific, we consider a system of N hard spheres of diameter σ_+ carrying charges $+q$, and N of diameter σ_- carrying charges $-q$. The interaction energy between two nonoverlapping ions, i and j, of charges q_i and q_j $(= \pm q)$ separated by distance r_{ij} is $U_{ij} = q_i q_j/D r_{ij}$, where D represents the dielectric constant of the solvent which will be set to unity. The hard-sphere interactions are supposed additive so that the $(+,-)$-ion collision diameter is $\sigma_\pm = \frac{1}{2}(\sigma_+ + \sigma_-)$. This, in fact, provides the basic length scale appropriate for defining both the reduced temperature and the reduced density via

$$T^* = k_B T D \sigma_\pm/q^2 \quad \text{and} \quad \rho^* = \rho \sigma_\pm^3, \tag{1}$$

[2,4] where $\rho = 2N/V$ is the *total* ionic number density. Other definitions of the reduced density are, of course, viable [3,10] and might be advantageous at high densities. However, at the low densities of interest here $(2\rho_c^* \lesssim 0.2)$ the formation of ion pairs, triples, chains, and rings (see Fig. 4) is controlled almost exclusively by $\sigma_\pm$, which remains well defined even if σ_+ or σ_- vanishes yielding point ions [14]. The reduced simulation box length is defined similarly via $L^* = L/\sigma_\pm$.

The key parameter for our study is the ratio of diameters of positive and negative ions, namely,

$$\lambda = \sigma_-/\sigma_+ . \tag{2}$$

Because of symmetry with respect to the exchange of + and − ions, only $\lambda \geq 1$ need by considered.

In addition to the ionic systems, we have studied, for the sake of comparison [15], tightly tethered dipolar dimer systems consisting of N pairs of a positive and a negative ion restricted to remain at separations σ_d satisfying $\sigma_\pm \leq \sigma_d \leq 1.02\sigma_\pm$. Interactions of the tethered dimers are otherwise identical to those of the ions.

We adopt the methodology of [12]. Neutral grand-canonical fine-discretization Monte Carlo simulations (characterized by a temperature T and a chemical potential for a pair of unlike ions, μ) have been performed on cubic boxes of length L, under periodic boundary conditions. The positions available to each ion are the sites of a simple cubic lattice of spacing a. A "lattice refinement" parameter $\zeta = \sigma_\pm/a$ is introduced, so that when $\zeta \to \infty$ the continuum is recovered. For values of $\zeta \geq 3$, the RPM displays a gas-liquid coexistence curve that approaches the continuum case quite closely already for $\zeta = 5$ [12]. In a Lennard-Jones fluid studied using $\zeta = 10$, the phase envelope and critical points of the lattice and continuum systems were equal within the simulation uncertainties

 0031-9007/00/85(21)/4558(4)$15.00

TABLE I. Critical parameters, $T_c^*(L^*)$ and $\rho_c^*(L^*)$, for the $\lambda = 1$, $\zeta = 10$ ionic models with two values of ϵ_∞. (The 1σ statistical uncertainties refer to the last decimal place.)

L^*	$100T_c^*$: $\epsilon_\infty = 1$,	$\epsilon_\infty = \infty$.	$100\rho_c^*$: $\epsilon_\infty = 1$,	$\epsilon_\infty = \infty$.
12	5.09(1)	4.97(1)	7.0(3)	8.0(2)
15	5.03(1)	4.96(1)	7.0(2)	8.2(3)
18	5.00(1)	4.96(1)	7.4(2)	7.9(2)

[16]. The structure of the liquid at short distances, as judged by the pair correlations, was also the same.

We have thus adopted a refinement parameter of $\zeta = 10$. For the largest value of λ we explore, namely, $\lambda \simeq 5\frac{2}{3}$, the diameter of the smaller sphere is $\sigma_+ = 3a$. When $\lambda = 1$, typical correlation functions for both like and unlike ion pairs then agree to within graphical accuracy with the corresponding continuum results (for the same T^*, ρ^*, and L^*). For higher values of λ (>1), the discretization effects on the $(+,-)$ and $(-,-)$ correlation functions decrease, while those on the $(+,+)$ correlation functions increase, as σ_+/a becomes smaller; but the latter are very small at short distances because of the strong repulsions.

The fine-lattice technique embodies precomputation and subsequent lookup of the Coulomb interaction between any two lattice sites, including all periodic images. The Ewald sums were performed with conduction ("tin-foil") boundary conditions, i.e., $\epsilon_\infty = \infty$; but for $\lambda = 1$, vacuum boundary conditions ($\epsilon_\infty = 1$) were also used to allow comparisons with [6]; see Table I and below.

Biased insertions and deletions of pairs of unlike ions were performed for ionic models, following [4]. Our tethered dimers have 318 distinct configurations on the lattice. Dimers were inserted by randomly placing the $-$ ion and selecting one of the 318 positions for the $+$ ion.

Histogram reweighting techniques were used to obtain the vapor-liquid envelopes up to $T \lesssim 0.98T_c$ [17]. Effective critical points for given L^* were estimated using mixed-field finite-size scaling methods [18], assuming Ising-type criticality. To discern a systematic dependence on λ, this approach should be satisfactory even though recent results [19] (which indicate that the pressure should also enter the field mixing) cast doubts on its full reliability.

The two Ewald-sum boundary conditions for $\lambda = 1$ yield different critical values (see Table I) but extrapolation to $L^* = \infty$ gives $T_c^* = 0.0495(2)$ for both cases and $\rho_c^* = 0.078(5)$ for $\epsilon_\infty = 1$ and 0.079(5) for $\epsilon_\infty = \infty$. The agreement is excellent; but since the $\epsilon_\infty = \infty$ results vary less with L^* they were used for the further simulations.

These $\lambda = 1$ results should approximate well those of the continuum RPM: recent studies [5–7] yield 0.0488(2)–0.0490(3) for T_c^* and 0.062(5)–0.080(5) for ρ_c^*. Our 1% larger value of T_c^* may be due to lattice discretization. Indeed, previous simulations [12] found that both $T_c^*(L^*)$ and $\rho_c^*(L^*)$ estimates decreased slightly as ζ increased.

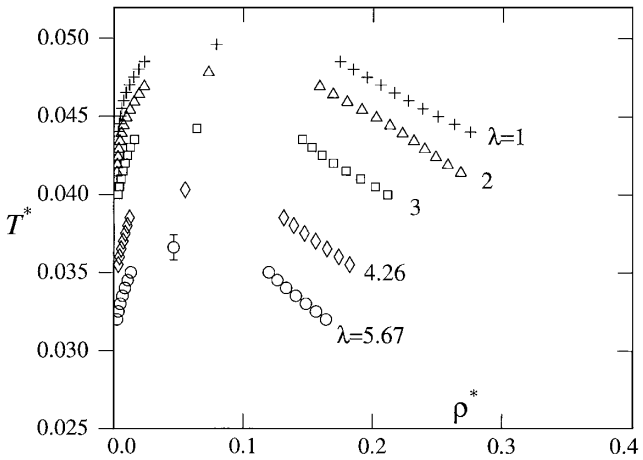

FIG. 1. Phase diagrams for ionic systems with various size asymmetries $\lambda = \sigma_-/\sigma_+$. Statistical uncertainties are shown only when larger than symbol sizes.

The calculated phase diagrams for the ionic and tethered dimer systems are shown in Figs. 1 and 2, respectively. The critical points, which are listed in Table II, were calculated [18] using $L^* = 18$ data while the subcritical coexistence curves were obtained using $L^* = 12$. The effects of size asymmetry are clearly strong, displaying a marked downward shift in T_c^* and ρ_c^* as λ increases. (The lower values of T_c^* result in smaller Monte Carlo acceptance ratios and increasing sampling difficulties.)

For $\lambda = 1$, the critical temperatures of the ionic and dimer systems seem almost identical. Indeed, although ρ_c is about 37% higher, the overall phase behavior of the dimers is quite similar to that of the ionic systems, as stressed by Shelley and Patey [15]. When λ increases, the critical temperatures of the dimers fall more rapidly but the critical densities approach those for ions, differing by only 11% at $\lambda \simeq 5.67$; see Fig. 3 where these results are depicted graphically versus the asymmetry parameter $\omega(\lambda) \equiv (1-\lambda)^2/(1+\lambda^2)$. This parameter respects the symmetry under exchange of $+$ and $-$

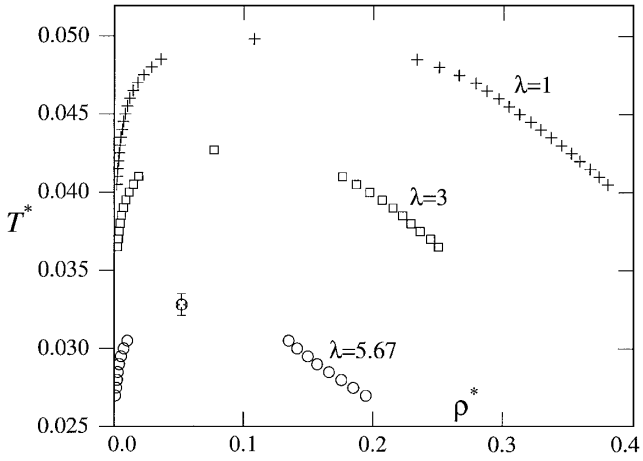

FIG. 2. Phase diagrams for tethered dipolar dimers.

TABLE II. Dependence on λ of estimated critical parameters for (a) ionic and (b) tethered dimer models.

λ	$T_c^* \times 10^2$	$-\mu_c^*$	$\rho_c^* \times 10^2$
(a) 1	4.96(1)	1.3424(1)	7.9(2)
2	4.79(1)	1.3347(1)	7.3(2)
3	4.42(1)	1.3189(1)	6.4(4)
4.26	4.03(2)	1.3009(4)	5.5(3)
5.67	3.66(8)	1.2880(8)	4.6(1)
(b) 1	4.98(1)	1.3210(1)	10.8(3)
3	4.27(1)	1.3005(1)	7.7(2)
5.67	3.28(7)	1.2795(4)	5.2(3)

ions and increases monotonically from $\omega(1) = 0$ for the RPM, up to $\omega(\infty) = 1$, for point ions. Extrapolating our data to the point-ion limit, $\omega = 1$, suggests a possibly common critical density, ρ_c^*, for ions and dimers of $\sim$0.015, with distinct critical temperatures, T_c^*, in the ranges 0.020–0.025 and 0.012–0.018. To check these speculations, however, may not be easy.

Also shown in Fig. 3, as crosses, are the predictions of the MSA (using the energy route) for $\lambda = 1, 2, 10$, and ∞ [2]. The absolute differences in T_c^* and ρ_c^* were to be anticipated (see, e.g., [20]); but it is striking that the predicted changes with λ in both T_c^* and ρ_c^* are *opposite* to those revealed by the simulations. The same failure to predict the correct trends is seen in the various calculations of Raineri *et al.* [3] as illustrated by the solid curves in Fig. 3. These derive from extensions of the Ebeling and Grigo theory (which employs Bjerrum ion pairing). (See also [20].)

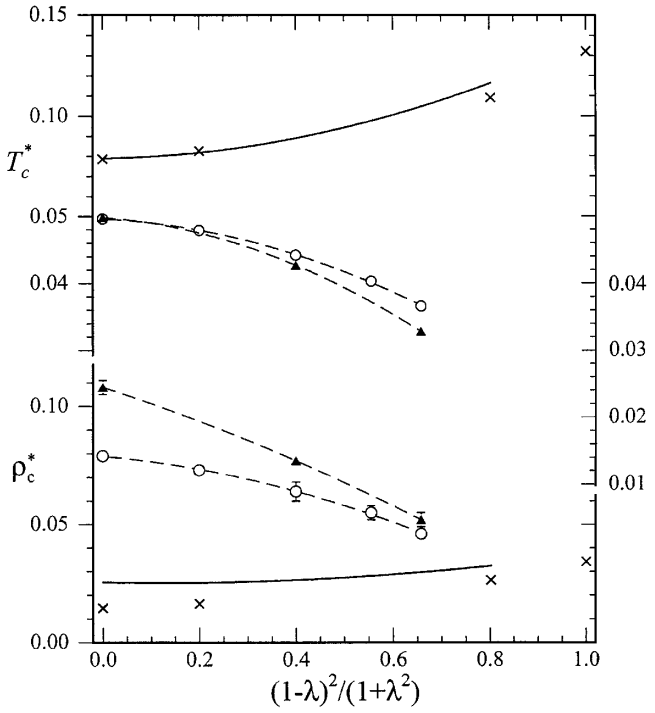

FIG. 3. Reduced critical temperatures T_c^* and densities ρ_c^* as functions of the asymmetry parameter, $\omega(\lambda) = (1 - \lambda)^2/(1 + \lambda^2)$, as found by simulations (i) for ionic systems (open circles) and (ii) for tethered dimers (solid triangles); and as predicted by theory using (iii) the MSA (energy route) [2] (crosses) and (iv) extended Ebeling-Grigo theory (in the EG-Eb approximation) [3] (solid lines).

The conflict of our data with the theories cited is, perhaps, not so surprising when one recognizes the large degree of pair association that occurs already in the critical region of the RPM ($\lambda = 1$) [20–22]. Indeed, the presence of many such closely coupled dipolar pairs is what motivated the comparison with charged dumbbells [15] and our tethered dimer systems. But, as realized for some time [14,21,23] and evident in sample configurations such as that in Fig. 4, dipolar systems undergo significant aggregation, primarily forming $(+, -)$ chains or "living polymers." Theories which mainly address the pair correlations cannot readily do justice to the geometrical aspects of the formation and interaction of such chains [23].

Conversely, some insight into the lowering of T_c^* as λ increases may be gained by examining how the ground-state binding energies, $E_b^* = E_b D\sigma_\pm/q^2$, of various specific configurations depend on λ. Thus for a neutral cluster of four ions (or two dipolar dimers) we find $E_b^* = 2.586$ for a square "ring" when $1 \le \lambda \le 1 + \sqrt{2}$; but E_b^* falls smoothly when λ exceeds 2.414 until, at $\lambda \simeq 8.26$, the lowest energy configuration switches from a planar diamond to a straight chain with $E_b^* = 2.333$. Similarly, if two long $(+, -)$ chains are brought together, the excess binding energy per ion is $E_b^* \simeq 0.752$ when $1 \le \lambda \le 2.414$ but decreases smoothly to 0.698 when λ grows larger. Other examples exhibit similar effects again rationalizing the observed drop in $T_c^*(\lambda)$.

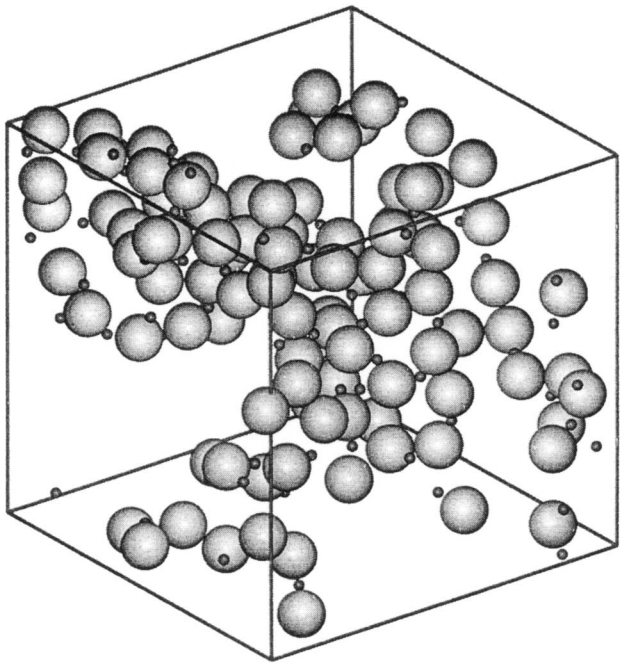

FIG. 4. Snapshot of an ionic configuration with $\lambda = 5\frac{2}{3}$ and $L^* = 15$ at $T^* = 0.0374 \simeq 1.02T_c^*$ and instantaneous density $\rho^* = 0.059 \simeq 1.27\rho_c^*$.

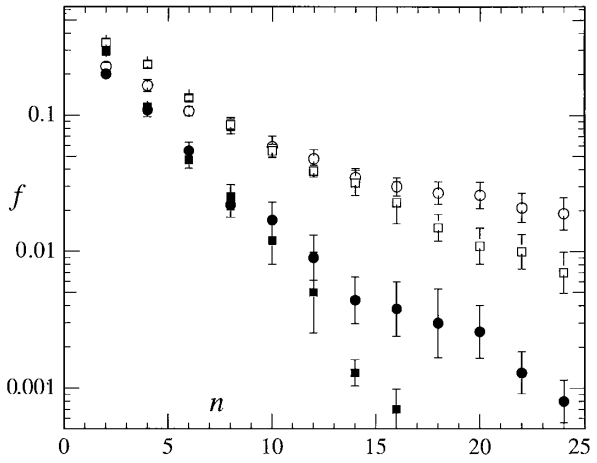

FIG. 5. Fraction f of ions in neutral clusters of n charged spheres in systems of size $L^* = 18$ at $\rho^* = \frac{1}{3}\rho_c^*$. Solid symbols denote ionic systems, open symbols tethered dipolar dimers. The squares correspond to symmetric ($\lambda = 1$) systems at $T^* = 0.050$, the circles to $\lambda = 3$ systems at $T^* = 0.045$. From the top downwards (at $n > 10$) the reduced densities are $\rho^* = 0.026$, 0.033, 0.019, and 0.027.

The fact that tethered dimers show lower T_c^* values (for $\lambda > 1$) than ionic systems supports the view that *free ions* assist in lowering the liquid free energy [20]. The result that the dimers require larger densities to stabilize the liquid is likewise consistent with this idea. In that connection the theory of [20], in which dipolar dimers are solvated by $+$ and $-$ free ions (which strongly screen opposite ends of a dimer), may reasonably be regarded as approximating the solvation of a dipolar dimer by other *dimers*: these will screen by orienting in head-to-tail fashion. A better theory is much to be desired but, as various attempts illustrate (see, e.g., [24]), that goal seems elusive.

Finally, in an attempt to quantify some structural differences between ionic and tethered dimer systems, cluster densities were sampled for selected, comparable conditions: see Fig. 5. Gillan's definition of a cluster [21] was used with a clustering distance $R_C^* = R_C/\sigma_{\pm} = 1.1$. It is evident that there are more large clusters in the less symmetric systems. But tethered dimers have much higher fractions of large clusters than do ionic systems, even allowing for the absence of charged clusters in the former.

In summary, our fine-discretization simulations of hard-core 1:1 electrolyte models have provided unequivocal evidence that increasing the size asymmetry, measured by the diameter ratio $\lambda = \sigma_-/\sigma_+$, leads to sharp, monotonic drops in appropriately scaled critical temperatures and densities [see (1)]. Tightly tethered dipolar dimers (or dumbbells [15]) display broadly similar behavior but with relatively larger critical densities, and critical temperatures that decrease faster with increasing λ. These trends are in severe disagreement with current theories [2,3] and present what appear to be deep challenges to our theoretical understanding even at a qualitative level.

We thank G. Stell, J. J. de Pablo, L. F. Rull, and G. Jackson for discussions and Professor Stell for providing a preprint of his work. Funding by the Department of Energy, Office of Basic Energy Sciences (DE-FG02-98ER14858, A. Z. P.) and the National Science Foundation (Grant No. CHE 99-81772, M. E. F.) is gratefully acknowledged. J. M. R.-E. acknowledges an FPI scholarship and Grant PB97-0712 from DGESIC, Spain.

Note added.—After this manuscript was submitted, we received a copy of Ref. [25] describing calculations for size-asymmetric electrolytes in the continuum. Critical temperatures and densities are in agreement, within statistical uncertainties, with results from the present work.

*Present address: Departamento de Fisica Atomica, Molecular y Nuclear, Universidad de Sevilla, 41080 Sevilla, Spain.
†Corresponding author.
Present address: Department of Chemical Engineering, Princeton University, Princeton, NJ 08544.
Email address: azp@princeton.edu

[1] M. Kleemeier *et al.,* J. Chem. Phys. **110**, 3085 (1999).
[2] E. Gonzalez-Tovar, Mol. Phys. **97**, 1203 (1999).
[3] F. O. Raineri, J. P. Routh, and G. Stell, J. Phys. IV (France) **10**, 99 (2000).
[4] G. Orkoulas and A. Z. Panagiotopoulos, J. Chem. Phys. **101**, 1452 (1994).
[5] J. M. Caillol *et al.,* J. Chem. Phys. **107**, 1565 (1997).
[6] G. Orkoulas and A. Z. Panagiotopoulos, J. Chem. Phys. **110**, 1581 (1999).
[7] Q. Yan and J. J. de Pablo, J. Chem. Phys. **111**, 9509 (1999).
[8] P. W. Debye and E. Hückel, Phys. Z. **24**, 185 (1923).
[9] D. M. Zuckerman, Ph.D. thesis, University of Maryland, 1998); D. M. Zuckerman, M. E. Fisher, and S. Bekiranov (to be published).
[10] A. K. Sabir *et al.,* Mol. Phys. **93**, 405 (1998).
[11] L. Belloni, Phys. Rev. Lett. **57**, 2026 (1986).
[12] A. Z. Panagiotopoulos and S. K. Kumar, Phys. Rev. Lett. **83**, 2981 (1999).
[13] A brief report was presented on 11 December 1999 at the 82nd Statistical Mechanical Conference at Rutgers University.
[14] M. J. Gillan, B. Larsen, M. P. Tosi, and N. H. March, J. Phys. C **9**, 889 (1976).
[15] J. C. Shelly and G. N. Patey, J. Chem. Phys. **103**, 8299 (1995).
[16] A. Z. Panagiotopoulos, J. Chem. Phys. **112**, 7132 (2000).
[17] A. M. Ferrenberg and R. H. Swendsen, Phys. Rev. Lett. **61**, 2635 (1988); **63**, 1195 (1989).
[18] N. B. Wilding and A. D. Bruce, J. Phys. Condens. Matter **4**, 3087 (1992).
[19] M. E. Fisher and G. Orkoulas, Phys. Rev. Lett. **85**, 696 (2000).
[20] Y. Levin and M. E. Fisher, Physica (Amsterdam) **225A**, 164 (1996), and references therein.
[21] M. J. Gillan, Mol. Phys. **49**, 421 (1983).
[22] P. J. Camp and G. N. Patey, Phys. Rev. E **60**, 1063 (1999).
[23] See J. M. Tavares, M. M. Telo da Gama, and M. A. Osipov, Phys. Rev. E **56**, R6252 (1997), and references therein.
[24] B. Guillot and Y. Guissani, Mol. Phys. **87**, 37 (1996).
[25] Q. Yan and J. J. de Pablo (to be published).